Perfect drain for the Maxwell fish eye lens

Juan C González[1], Pablo Benítez and Juan C Miñano

Universidad Politécnca de Madrid, Cedint Campus de Montegancedo,
28223 Madrid, Spain
E-mail: jcgonzalez@cedint.upm.es

Abstract. Perfect imaging of electromagnetic waves using the Maxwell fish eye (MFE) requires a new concept: a point called the perfect drain that we shall call the *perfect point drain*. From the mathematical point of view, a *perfect point drain* is just like an ideal point source, except that it drains power from the electromagnetic field instead of generating it. We introduce here the *perfect drain* for the MFE as a dissipative region of non-zero size that completely drains the power from the point source. To accomplish this goal, the region must have a precise complex permittivity that depends on its size as well as on the frequency. The *perfect point drain* is obtained when the diameter of the *perfect drain* tends to zero. This interpretation of the *perfect point drain* is connected well with common concepts of electromagnetic theory, opening up both modeling in computer simulations and experimental verification of setups containing a *perfect point drain*.

S Online supplementary data available from stacks.iop.org/NJP/13/023038/mmedia

[1] Author to whom any correspondence should be addressed.

Contents

1. Introduction

The possibility of focusing light below the diffraction limit (super-resolution) has been demonstrated during the last decade using left-handed materials [1]–[4] (i.e. materials with negative dielectric and magnetic constants [5]). Recently, a new possibility has been introduced for a material with a positive, isotropic and inhomogeneous refractive index. This possibility uses the Maxwell fish eye (MFE) lens. It is well known that, in the geometrical optics (GO) framework, the MFE perfectly focuses rays emitted by an arbitrary point of space into another (its image point). Leonhardt [6] has demonstrated that the MFE lens in two dimensions (2D) not only perfectly focuses radiation in the GO approximation, but also does so for actual fields of any frequency, a result that has been confirmed via a different approach [7]. This 2D analysis describes TE-polarized light in a cylindrical medium (where the electric field vector **E** points orthogonal to the plane), and the electric field magnitude fulfills the Helmholtz equation. Leonhardt and Philbin [8] have also demonstrated the analogous ideality of a novel impedance-matched spherical MFE for perfect focusing of electromagnetic waves in 3D.

In the 2D case, the perfect focusing of the MFE in [6] ensures that the medium will perfectly transport an outward (monopole) Helmholtz wave field, one generated by a point source, towards an 'infinitely well localized drain' [6] (one that we will call '*perfect point drain*') located at the desired image point. Note that the *perfect point drain* must be such that it totally absorbs all incident radiation, with no reflection or scattering by it. Note also that the field around the drain asymptotically coincides with an inward (monopole) wave. Here we will refer to such a wave as 'Leonhardt's forward wave'.

Even though the physical significance of a point source as a limiting case seems to be well accepted, that of a passive perfect point drain has been considered very controversial [9]–[12]. In [6], the drain was not physically described, but only considered as a mathematical entity,

leaving no clues as to how to simulate that drain in software or how to make it. In particular, an analysis of such a drain, one located at a position different from the image point, would help one to prove the super-resolution, which could not be done with the information in [6].

Recently, however, a candidate for a perfect drain has been proposed for a microwave-frequency MFE [13], wherein a 2D MFE medium has been assembled as a planar waveguide with concentric layers of copper circuit board forming the desired refractive index profile of the MFE. Also, both the source and the drain have been built as identical coaxial probes, one to introduce power into the planar waveguide and the other to extract it. The coaxial probe was intended to act as the perfect sink and is completely passive and loaded with the characteristic impedance of the coaxial cable [13]. There is no theoretical proof that such a coaxial probe will actually behave as a perfect drain, but a practical proof is claimed by comparing (figure 4 in [13]) the measured electric field distribution and the analytical expression for Leonhardt's forward wave ([6], reviewed here in section 1.1). Since the measured and analytical values differ significantly (deviations attributed primarily to imperfections in the probes), we think a more detailed analysis is called for in order to clarify whether or not that receiving coaxial probe is acting as the perfect drain as defined here. Nevertheless, this clarification does not affect the main conclusion in [13]: such a probe certainly leads to super-resolution in the conditions of that measurement.

In this paper, we present a different realization of a passive perfect drain, obtained theoretically from analytical equations. It consists in the introduction of a certain non-magnetic material inside a circle of radius R enclosing the image point (although not centered upon it, as discussed later). As will be proved in section 2, the complex permittivity of that non-magnetic material will be such that the field outside that circle coincides exactly with Leonhardt's forward wave and the incoming power will be fully absorbed inside it. In general, this perfect drain can have a finite radius R; the *perfect point drain* is just the limit case when $R \to 0$.

1.1. Leonhardt's forward wave

The strength of the TE monochromatic field $E(x, y)e^{-i\omega t}\mathbf{z}$ in a region without sources or drains fulfils the 2D Helmholtz equation,

$$\Delta E + n^2 k_0^2 E = 0, \tag{1}$$

where $k_0 = \omega\sqrt{\mu_0 \varepsilon_0}$ and n is the MFE refractive index distribution given by

$$n = \frac{2}{1 + \rho^2}, \tag{2}$$

where $\rho = \sqrt{x^2 + y^2}$. Leonhardt's forward wave is a particular family of solutions of equation (1), given by equation (12) of [6],

$$E = \frac{P_\nu(\zeta) - e^{i\nu\pi} P_\nu(-\zeta)}{4\sin(\nu\pi)}, \tag{3}$$

where P_ν is the Legendre function of the first kind,

$$\nu = \frac{-1 + \sqrt{1 + 4k_0^2}}{2}, \tag{4}$$

and

$$\zeta = \frac{|z'|^2 - 1}{|z'|^2 + 1}, \quad z' = \frac{z - x_0}{z\,x_0 + 1}. \tag{5}$$

Here, $z = x + \mathrm{i}y$ is the complex notation of the point (x, y), and x_0 is an arbitrary real number. Without lack of generality, we have located the point source described in [5] at the object point $(x_0, 0)$. Note that $-1 \leqslant \zeta \leqslant 1$ and by the divergence of $P_\nu(\zeta)$ when $\zeta \to -1$, E is infinite at $|\zeta| = 1$. A wave according to equation (3) is generated by the point source located at $(x_0, 0)$, and it propagates towards the perfect point drain at the image point $(-1/x_0, 0)$. The time evolution of the field, $\mathrm{Re}(E(x, y)\mathrm{e}^{-\mathrm{i}\omega t})$, is shown in the associated media files, Movies 1 and 2 (available in the supplementary data, at stacks.iop.org/NJP/13/023038/mmedia), for $x_0 = -2$, $k = 15$. This evolution clearly includes the one-directional propagation of the wave from the source to the drain, with no reflection or scattering by it.

The magnetic field $\mathbf{H}(x, y)$ of Leonhardt's forward wave can be easily computed from the field $\mathbf{E}$, equations (3) and (5), as

$$\mathbf{H} = \frac{1}{\mathrm{i}\omega\mu}\nabla \times \mathbf{E} = \frac{1}{\mathrm{i}\omega\mu}\frac{\mathrm{d}E}{\mathrm{d}\zeta}\left(\frac{\partial\zeta}{\partial y}\mathbf{x} - \frac{\partial\zeta}{\partial x}\mathbf{y}\right). \tag{6}$$

1.2. Current of the source

Equation (1) is only valid in a region without sources or drains, in our case the full plane except for the points $(x_0, 0)$ and $(-1/x_0, 0)$. An equation valid for the full plane must include the Dirac delta at those points. The amplitude of equation (3) was specifically selected in [6] to make it behave as a Green's function, so the weights of those Dirac deltas have unit modulus. It can be written as [6]–[8]

$$\Delta E + n^2 k_0^2 E = -\delta(x - x_0, y) - \mathrm{e}^{\mathrm{i}\nu\pi}\delta(x + 1/x_0, y). \tag{7}$$

The right-hand side of equation (7) can be identified (from the Maxwell equations) as $-\mathrm{i}\omega\mu\, J(x, y)z$, where $J(x,y)$ is the current density. Consequently, the electric currents through the source and the drain for the specific field amplitude of equation (3) are

$$I_{\mathrm{source}} = \frac{1}{\mathrm{i}\omega\mu_0}, \quad I_{\mathrm{drain}} = \frac{\mathrm{e}^{i\pi\nu}}{\mathrm{i}\omega\mu_0} = \mathrm{e}^{i\pi\nu}I_{\mathrm{source}}. \tag{8}$$

1.3. Alternative expression for the forward wave

There is an alternative way to express equation (3) (equation (12) of [6]), which uses the Legendre function of the second kind Q_ν. We consider here the branch of Q_ν that is real valued when $\mathrm{Im}(\zeta) = 0$ and $|\zeta| < 1$ (another complex-valued branch Q_ν is claimed to be considered in [6]). Taking into account, from [14] (equation (15) on p 144), that

$$P_\nu(-\zeta) = \cos(\pi\nu)P_\nu(\zeta) - \sin(\pi\nu)\frac{2}{\pi}Q_\nu(\zeta), \tag{9}$$

equation (3) can be alternatively rewritten, with the help of (9), as

$$E = \frac{-\mathrm{i}\mathrm{e}^{\mathrm{i}\pi\nu}}{4}\left[P_\nu(\zeta) + \mathrm{i}\frac{2}{\pi}Q_\nu(\zeta)\right]. \tag{10}$$

Let us represent the factor in square brackets of (10) by

$$F_\nu(\zeta) = P_\nu(\zeta) + \mathrm{i}\frac{2}{\pi}Q_\nu(\zeta). \tag{11}$$

Interesting asymptotic expressions for function F_ν are set forth in appendix 1, which gives a comprehensive discussion of Leonhardt's forward wave. Additionally, this alternative expression will greatly simplify some calculations in the perfect sink design of the next section.

2. Perfect sink

The theoretically ideal point drain of Leonhardt is located at point $(-1/x_0, 0)$. We will design first a finite-area perfect drain, which will comprise a convex region surrounding that point $(-1/x_0, 0)$, filled with an inhomogeneous, isotropic, non-magnetic material with complex dielectric permittivity (thus absorptive), such that the field outside that region coincides exactly with Leonhardt's forward wave.

The equation satisfied by the field in that region will then be the homogeneous Helmholtz equation. Since the incident wave fields E and H are known, the necessary continuity of E and H on the drain boundary will be forced by particularizing on the boundary the values of E and H in equations (3) and (6), respectively.

2.1. Selection of the boundary

From equation (5), it is easy to confirm that the line $\zeta = \zeta_d = $ constant is a circle with its center at point $(x_c, 0)$ and its radius R given by

$$x_c = \frac{2x_0}{1 - x_0^2 - (1 + x_0^2)\zeta_d}, \qquad R = \frac{-\sqrt{1 - \zeta_d^2}(1 + x_0^2)}{1 - x_0^2 - (1 + x_0^2)\zeta_d}. \tag{12}$$

We select the drain region as that containing the points fulfilling $\zeta \geqslant \zeta_d$, with ζ_d fulfilling

$$\zeta_d > \frac{1 - |x_0|^2}{1 + |x_0|^2}. \tag{13}$$

Condition equation (13) is required in order to guarantee that the drain area is finite and encloses the image point $(-1/x_0, 0)$, as can be deduced from equation (12). The $\zeta = $ constant circumferences are shown in red in figure 1. The $\zeta = $ constant circumferences are also $E = $ constant lines (see equation (3)) and coincide with the GO wavefronts. This property is fulfilled by a more general class of inhomogeneous media, a class analyzed in [7]. The blue lines in figure 1, which we can call $\delta = $ constant, are also circumferences. They coincide with the GO rays and are the Poynting vector lines of Leonhardt's forward wave. Both families of lines coincide with coordinate grid lines of the bipolar orthogonal coordinate system (see for instance [7]).

From equation (12) we see that selecting ζ_d close enough to 1 will make the radius R as small as desired. At the limit $\zeta_d \to 1$, we obtain the *perfect point drain* $(R \to 0, x_c \to -1/x_0)$.

2.2. Inhomogeneous complex refractive index of the drain

Inside the drain $(\zeta \geqslant \zeta_d)$, we select $\mu = \mu_0$ and the refractive index has the following form,

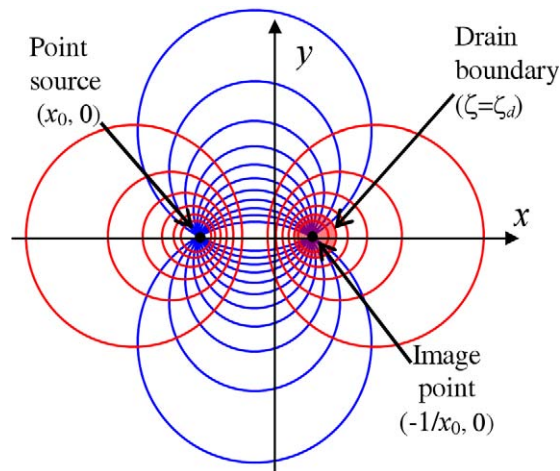$$n_d = \frac{2\sqrt{\varepsilon_d}}{1 + \rho^2}, \tag{14}$$

Figure 1. Source, drain and cylindrical bipolar coordinate system in MFE. The source is a line of current perpendicular to the *x*–*y* plane and placed at the point $(x_0, 0)$, which defines the 2D point source. The boundary of the finite-area passive drain is a cylinder with base $\zeta > \zeta_d$. The red lines ($\zeta =$ constant) and the blue lines ($\delta =$ constant) define a cylindrical bipolar coordinate system.

where ε_d is a complex constant and with $\mathrm{Im}(\varepsilon_d) \neq 0$ to be calculated later (in section 3). Then, the homogeneous Helmholtz equation in the drain is

$$\Delta E + n_d^2 k_0^2 E = 0. \tag{15}$$

Define $k_d = \omega\sqrt{\mu_0\varepsilon_0\varepsilon_d}$ (which is complex). Using the expression for the refractive index *n* of the MFE (equation (2)), we find that the selection made with equation (14) fulfills that $n_d k_0 = n k_d$, so equation (15) can also be written as

$$\Delta E + n^2 k_d^2 E = 0. \tag{16}$$

This equation is identical to the Helmholtz equation of the MFE, equation (1), after substituting the real wave number k_0 by k_d (still to be calculated).

2.3. Ordinary differential equation of the drain

One of the boundary conditions on the line $\zeta = \zeta_d$ is the continuity of the field $\mathbf{E} = E\mathbf{z}$. As mentioned before, *E* is constant on that boundary surface, so it would be particularly interesting to express equation (16) in the bipolar coordinate system $\zeta-\delta$. That was already done in section 3.1 of [7]. As shown there, the expression of equation (16) for solutions depending only on ζ is the same as that of equation (9) in [6]. Using the change in variables $\zeta = (r^2 - 1)/(r^2 + 1)$, this equation is

$$\frac{1}{r}\frac{\mathrm{d}}{\mathrm{d}r}\left(r\frac{\mathrm{d}E}{\mathrm{d}r}\right) + n^2 k_d^2 E = 0. \tag{17}$$

Its general solution [14] can be written as

$$E = A\, P_{\nu'}(\zeta) + B\, Q_{\nu'}(\zeta), \tag{18}$$

IOP Institute of Physics ⬦DEUTSCHE PHYSIKALISCHE GESELLSCHAFT

where ν' is given by

$$\nu' = \frac{-1 + \sqrt{1 + 4k_d^2}}{2}. \tag{19}$$

The three constants A, B and ν' are fixed by three conditions. Two of them are given by the continuity of the **E** and **H** fields at the boundary, and the third is that the field E must be bounded (i.e. it cannot diverge), since the Helmholtz equation (15) is homogeneous.

   Consider first the third condition. From the properties of the Legendre functions [14], we know that the function $Q_{\nu'}(\zeta)$ diverges when $\zeta \to 1$, if $\mathrm{Im}(\nu') \neq 0$ and $P_{\nu'}(\zeta)$ do not ($P_{\nu'}(1) = 1$). Therefore, this boundary condition imposes $B = 0$, which means that the field inside the drain region ($\zeta \geqslant \zeta_d$) has the form

$$E = A\, P_{\nu'}(\zeta). \tag{20}$$

A and ν' are calculated, forcing the other two conditions, i.e. the continuity of **E** and **H** at the boundary. **E** and **H** outside the drain are taken from the solution in the absence of reversed wave (so the drain is reflectionless), i.e. by using equations (10) and (6).

$$A\, P_{\nu'}(\zeta_d) = -\mathrm{i}e^{\mathrm{i}\pi\nu}\left(P_\nu(\zeta_d) + \mathrm{i}\frac{2}{\pi} Q_\nu(\zeta_d) \right),$$

$$A\,\left.\frac{\mathrm{d}P_{\nu'}}{\mathrm{d}\zeta}\right|_{\zeta_d} = -\mathrm{i}e^{\mathrm{i}\pi\nu}\left(\left.\frac{\mathrm{d}P_\nu}{\mathrm{d}\zeta}\right|_{\zeta_d} + \mathrm{i}\frac{2}{\pi}\left.\frac{\mathrm{d}Q_\nu}{\mathrm{d}\zeta}\right|_{\zeta_d} \right). \tag{21}$$

Dividing both equations, we obtain

$$\frac{\left.\frac{\mathrm{d}P_{\nu'}}{\mathrm{d}\zeta}\right|_{\zeta_d}}{P_{\nu'}(\zeta_d)} = \frac{\left.\frac{\mathrm{d}P_\nu}{\mathrm{d}\zeta}\right|_{\zeta_d} + \mathrm{i}\frac{2}{\pi}\left.\frac{\mathrm{d}Q_\nu}{\mathrm{d}\zeta}\right|_{\zeta_d}}{P_\nu(\zeta_d) + \mathrm{i}\frac{2}{\pi} Q_\nu(\zeta_d)}, \tag{22}$$

which is an expression where only ν' is unknown. Once this is solved, we can calculate ε_d with equation (19). Equation (22) has been numerically solved with Wolfram Mathematica 7,

$$\varepsilon_d = \left(\frac{k_d}{\omega\sqrt{\mu_0\varepsilon_0}} \right)^2 = \frac{\nu'(\nu'+1)}{\omega^2\mu_0\varepsilon_0}. \tag{23}$$

3. Examples

Figure 2 shows ε_d of a *perfect drain* as a function of frequency for two different drain radii, and figure 3 shows it as a function of the drain radius for different frequencies. In all of the examples, we shall assume that ρ in equations (2) and (14) is given in cm and the frequency in GHz. Movies 3 and 4 (available at stacks.iop.org/NJP/13/023038/mmedia) show the time evolution of the field, $\mathrm{Re}(E(x,y)e^{-\mathrm{i}\omega t})$ for a drain radius $R = 0.2$ cm, $x_0 = -2$, $k = 15$. This should be compared with the case of the *perfect point drain* shown in the introduction (Movies 1 and 2). Movie 5 shows the time evolution of the field inside the drain for a radius of 0.2 cm.
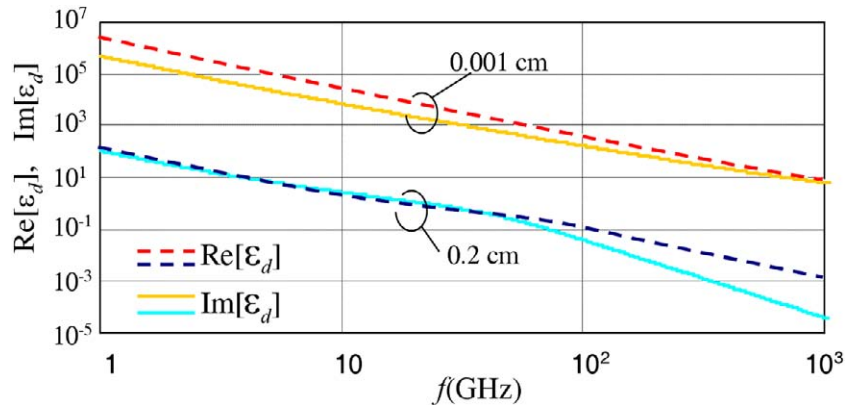
Figure 2. Dependence of the ε_d of a *perfect drain* on frequency. Dark and bright blue curves correspond to the real and imaginary parts for a drain radius of 0.2 cm centered at $x_c = 0.5159$ cm, $y_c = 0$. Red and orange curves correspond to the real and imaginary parts for a drain radius of 0.001 cm centered at $x_c = 0.5$ cm, $y_c = 0$. The point source is located at $x_0 = -2$ cm, $y_0 = 0$. The frequency is in GHz.
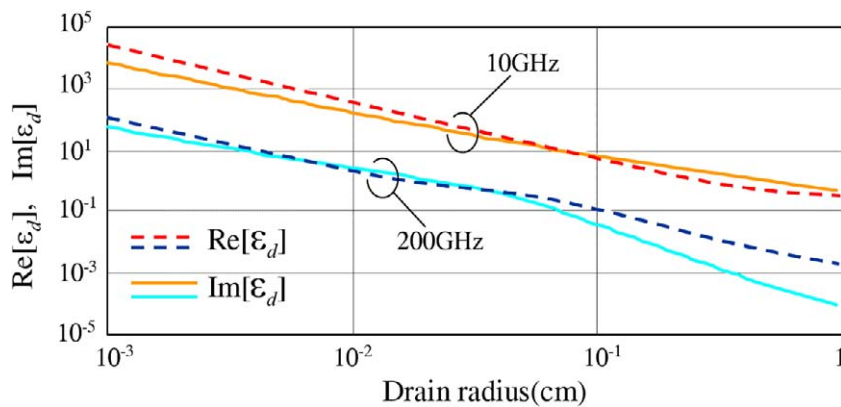

Figure 3. Dependence of the ε_d of a *perfect drain* on drain radius. Dark and bright blue curves correspond to the real and imaginary parts for a frequency of 200 GHz. Red and orange curves correspond to the real and imaginary parts for a frequency of 10 GHz.

4. Looking inside the drain

4.1. The electric field and current inside the drain

The conductivity σ of the media inside the drain can be calculated as a function of ε_d from its definition,

$$\sigma = \frac{\omega}{\mu_0} \mathrm{Im}[n_d^2 k_0^2] = \frac{4\omega\varepsilon_0}{(1+\rho^2)^2} \mathrm{Im}[\varepsilon_d]. \tag{24}$$
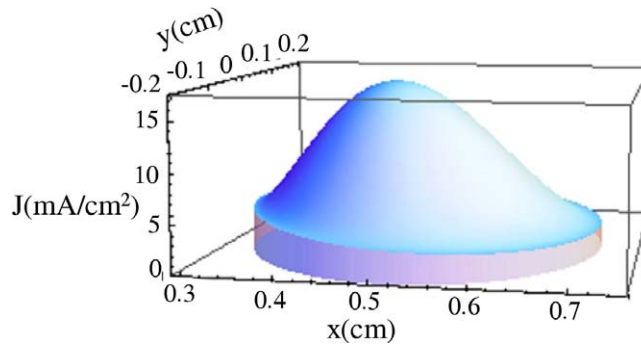
Figure 4. Representation of the modulus of the current density (mA cm^{-2}) inside the drain. Drain radius $= 0.2$ cm; the drain center is at $(0.519, 0)$ cm. The total current in the source is 1 mA.

Using equation (23), we can calculate σ as a function of ν'. The electric field inside the drain is given by equation (20). Consequently, the current density $\mathbf{J} = \sigma \mathbf{E}$ in the drain is

$$\mathbf{J}(x, y) = \frac{4A\omega\varepsilon_0}{(1+\rho^2)^2}\mathrm{Im}[\varepsilon_\mathrm{d}]P_{\nu'}(\zeta)\mathbf{z}. \tag{25}$$

Figure 4 shows the modulus of the current density inside the drain for a drain radius of 0.2 cm and a total current in the source of 1 mA when the drain center is at the point $(0.519, 0)$ cm.

4.2. Power absorption

The power emitted by the source P can be obtained by integrating the Poynting vector over a surface enclosing the source. The MFE is a lossless system, so this power has to equal both the total power entering the drain and the power that it absorbs. This integration has been made as shown in equation (26). This surface has cylindrical symmetry along the z-axis, so for the sake of simplicity we take a surface whose projection on the x–y plane is a $\zeta =$ constant curve, let us say $\zeta = \zeta_s$. Since the Poynting vector has no z-dependence, the surface integral is reduced to a line integral along $\zeta = \zeta_s$.

$$P = \frac{1}{2}\mathrm{Re}\left[\int \mathbf{E} \times \mathbf{H}^* \cdot \mathbf{dl}\right]$$

$$= \frac{1}{2}\mathrm{Re}\left[\left(P_\nu(\zeta_s) + \mathrm{i}\frac{2}{\pi}Q_\nu(\zeta_s)\right)\left(\frac{1}{\mathrm{i}\omega\mu}\frac{\mathrm{d}\left(P_\nu(\zeta) - \mathrm{i}\frac{2}{\pi}Q_\nu(\zeta)\right)}{\mathrm{d}\zeta}\bigg|_{\zeta_s}\right)^* \int_{\zeta=\zeta_s}\left(\frac{\partial\zeta}{\partial y}, -\frac{\partial\zeta}{\partial x}\right) \cdot \mathbf{dl}\right]. \tag{26}$$

Alternatively, the same power can be calculated as the power absorbed in the volume of the drain, which is

$$P = \frac{1}{2}\mathrm{Re}\left[\int \mathbf{J} \times \mathbf{E}^* \,\mathrm{d}V\right] = \frac{1}{2}\int_{\zeta \leqslant \zeta_\mathrm{d}}\sigma|AP_{\nu'}(\zeta)|^2\,\mathrm{d}S$$

$$= \frac{1}{2}\mathrm{Re}\left[|A|^2P_{\nu'}(\zeta_\mathrm{d})\left(\frac{1}{\mathrm{i}\omega\mu}\frac{\mathrm{d}P_{\nu'}(\zeta)}{\mathrm{d}\zeta}\bigg|_{\zeta_\mathrm{d}}\right)^*\right]\int_{\zeta=\zeta_\mathrm{d}}\left(\frac{\partial\zeta}{\partial y}, -\frac{\partial\zeta}{\partial x}\right) \cdot \mathbf{dl}. \tag{27}$$
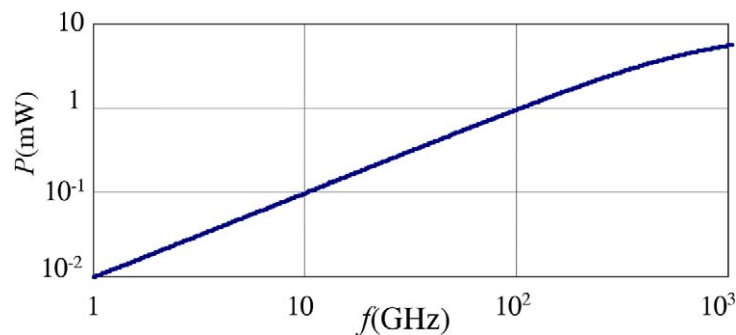
Figure 5. Power emitted by the source and absorbed by the drain as a function of frequency. The total current in the source is 1 mA.

Figure 5 shows the power P as a function of the frequency for 1 mA total current in the point source. Note that this implies an amplitude value for Leonhardt's forward wave, correspondingly scaled from equations (3) and (8). The power P depends on the source total current and frequency, but obviously it does not depend on the drain radius.

5. Conclusions

We have introduced the *perfect drain* concept as a region that absorbs all of the energy carried by Leonhardt's forward wave solution F_ν in the MFE, leading to a field solution where there is no reverse wave R_ν and consequently no reflected energy. This region has a specific complex permittivity that depends on frequency and on the drain radius (figures 2 and 3 show an example). Without such a *perfect drain*, both the forward and the reverse waves appear as responses to the point source. When the diameter of the *perfect drain* tends to zero, both the real and the imaginary parts of the corresponding permittivity tend to infinity, and the *perfect drain* becomes the *perfect point drain* introduced by Leonhardt, i.e. it tends to a region of zero diameter that completely absorbs the forward wave.

This result allows us to model and simulate a *perfect point drain* as a small (and finite) dissipative region. Unlike the *perfect point drain*, the model of a *perfect drain* with non-zero radius can easily be included in electromagnetic analysis software, and its experimental setup is readily realized. These two features simplify analysis and experimental verification of super-resolution in the MFE, i.e. checking that the power absorbed by the drain changes drastically when the drain moves to a neighboring point located at a distance much smaller than the wavelength from the source image point.

Acknowledgments

Appendix. Asymptotic expression when $v \gg 1$ and the reverse wave

Using equations (1) and (2) on p 162 of [14], the functions $P_v(\zeta)$ and $Q_v(\zeta)$, $\zeta = \cos\theta$, for $\varepsilon < \theta < \pi - \varepsilon$ ($\varepsilon > 0$) can be approximated as

$$P_v(\cos\theta) = \frac{\Gamma(v)}{\Gamma(v+3/2)}\sqrt{\frac{2}{\pi\sin\theta}}\{\cos((v+1/2)\theta) + O(v^{-1})\},$$

$$Q_v(\cos\theta) = \frac{\Gamma(v)}{\Gamma(v+3/2)}\sqrt{\frac{\pi}{2\sin\theta}}\{-\sin((v+1/2)\theta) + O(v^{-1})\}. \tag{A.1}$$

Thus, using equation (11), we have

$$F_v(\cos\theta) = \frac{\Gamma(v)}{\Gamma(v+3/2)}\sqrt{\frac{2}{\pi\sin\theta}}\{e^{-i(v+1/2)\theta} + O(v^{-1})\}, \tag{A.2}$$

which is clearly identified as a wave propagating toward decreasing values of θ (remember the factor $e^{-i\omega t}$), that is, increasing ζ, from the source to the drain. This expression is accurate for $\varepsilon < \theta < \pi - \varepsilon$ ($\varepsilon > 0$) (i.e. not too close to the point source and point drain). Asymptotes to equations (A.1) and (A.2) suggest defining the reverse function R_v,

$$R_v(\zeta) = P_v(\zeta) - \frac{2}{\pi}iQ_v(\zeta), \tag{A.3}$$

to describe a field propagating from the image point to the object point. In analogy to canonical solutions of the Helmholtz equation (as planar waves, cylindrical waves or spherical waves in free space), it seems more natural for this MFE problem to define the general solution of equation (17) as a superposition of the functions F_v and R_v, i.e. to rewrite the field E as

$$E = C\,F_v(\zeta) + D\,R_v(\zeta). \tag{A.4}$$

When there is a *perfect drain*, only Leonhardt's forward wave F_v exists in the region outside the circle delimiting the *perfect drain*, which implies that D in equation (A.4) is null. This means that there is no reverse wave going back to the source. Inside the *perfect drain* region, the condition that the field E must be bounded leads to equation (20), which in terms of $F_{v'}$ and $R_{v'}$ implies the condition $C = D$. This means that inside the *perfect drain* there is a standing wave, which is necessary in order to avoid the singularity at the image point ($\zeta = 1$). This is analogous to the superposition of converging and diverging cylindrical waves, of equal amplitude, in free space as described by the Hankel functions $H_0^{(1)}(k_0\rho)$ and $H_0^{(2)}(k_0\rho)$, which results in the bounded Bessel function $J_0(k_0\rho)$.

The forward and reverse waves defined here for the MFE lens are intimately related to the retarded and advanced fields defined in [12] and [13] for the MFE mirror. Using the formulation in [12] and [13], a wave bounded at the image point for the MFE lens can be written as

$$E = \frac{F_{v(k_0)} - e^{i\pi(v(k_0)-v(-k_0))}F_{v(-k_0)}}{1 - e^{i\pi(v(k_0)-v(-k_0))}}, \tag{A.5}$$

where the positive and negative wave numbers are defined as

$$v(\pm k_0) = \frac{-1 \pm \sqrt{1+4k_0^2}}{2}. \tag{A.6}$$

In addition to the complexity of the expression equation (A.5), it can easily be seen that it is (up to a multiplicative constant) simply equal to P_v (which is the bounded expression

used above in equation (20)). This is obtained by direct computation, after considering that $\nu(-k_0) = -\nu(k_0) - 1$, and then using equations (7) and (16) on p 144 of [14],

$$P_{-\nu-1}(\zeta) = P_\nu(\zeta),$$
$$Q_{-\nu-1}(\zeta) = -\pi \cot(\pi\nu) P_\nu(\zeta) + Q_\nu(\zeta). \tag{A.7}$$

References

[1] Pendry J B 2000 Negative refraction makes a perfect lens *Phys. Rev. Lett.* **85** 3966–89

[2] Shelby R A, Smith D R and Schultz S 2001 Experimental verification of negative index of refraction *Science* **292** 79

[3] Fang N, Lee H, Sun C and Zhang X 2005 Sub-diffraction-limited optical imaging with a silver superlens *Science* **308** 534–7

[4] Mesa F, Freire F, Marqués R and Baena J D 2005 Three dimensional superresolution in material slab lenses: experiment and theory *Phys. Rev.* B **72** 235117

[5] Veselago V G 1968 The electrodynamics of substances with simultaneously negative values of ε and μ *Sov. Phys.—Usp.* **10** 509–14

[6] Leonhardt U 2009 Perfect imaging without negative refraction *New J. Phys.* **11** 093040

[7] Benítez P, Miñano J C and González J C 2010 Perfect focusing of scalar wave fields in three dimensions *Opt. Express* **18** 7650–63

[8] Leonhardt U and Philbin T G 2010 Perfect imaging with positive refraction in three dimensions *Phys. Rev.* A **81** 011804

[9] Merlin R 2010 Comment on 'Perfect imaging with positive refraction in three dimensions' arXiv:1007.0280v2 [physics.optics]

[10] Leonhardt U and Bin T G 2010 Reply to the Comment on 'Perfect imaging with positive refraction in three dimensions' arXiv:1009.1766v1 [physics.optics]

[11] Blaikey R J 2010 Comments on Perfect imaging without negative refraction *New J. Phys* **12** 058001

[12] Leonhardt U and Philbin T G 2010 Reply to comments on Perfect imaging without negative refraction *New J. Phys.* **12** 058002

[13] Ma Y G, Ong C K, Sahebdivan S, Tyc T and Leonhardt U 2010 Perfect imaging without negative refraction for microwaves arXiv:10072530v1

[14] Erdélyi A, Magnus W, Oberhettinger F and Tricomi F G 1953 *Higher Transcendental Functions* vol I (New York: McGraw-Hill)